DOI: 10.1002/cbic.200700569

Structural, Functional and Calorimetric Investigation of MosA, a Dihydrodipicolinate Synthase from *Sinorhizobium meliloti* L5–30, does not Support Involvement in Rhizopine Biosynthesis

Christopher P. Phenix,[a, c] Kurt Nienaber,[b] Pui Hang Tam,[a, b, d] Louis T. J. Delbaere,[b] and David R. J. Palmer*[a, b]

MosA is an enzyme from Sinorhizobium meliloti *L5–30, a beneficial soil bacterium that forms a symbiotic relationship with leguminous plants. MosA was proposed to catalyze the conversion of* scyllo*-inosamine to 3-*O*-methyl-*scyllo*-inosamine (compounds known as rhizopines), despite the MosA sequence showing a strong resemblance to dihydrodipicolinate synthase (DHDPS) sequences rather than to methyltransferases. Our laboratory has already shown that MosA is an efficient catalyst of the DHDPS reaction. Here we report the structure of MosA, solved to 1.95 Å resolution, which resembles previously reported DHDPS structures. In this structure Lys161 forms a Schiff base adduct with pyruvate, consistent with the DHDPS mechanism. We have synthesized both known rhizopines and investigated their ability to interact with MosA in the presence and absence of methyl donors. No MosA-catalyzed methyltransferase activity is observed in the presence of* scyllo*-inosamine and S-adenosylmethionine (SAM). 2-Oxobutyrate can form a Schiff base with MosA, acting as a competitive inhibitor of MosA-catalyzed dihydrodipicolinate synthesis. It can be trapped on the enzyme by reaction with sodium borohydride, but does not act as a methyl donor. The presence of rhizopines does not affect the kinetics of dihydrodipicolinate synthesis. Isothermal titration calorimetry (ITC) shows no apparent interaction of MosA with rhizopines and SAM. Similar experiments with pyruvate as titrant demonstrate that the reversible Schiff base formation is largely entropically driven. This is the first use of ITC to study Schiff base formation between an enzyme and its substrate.*

Introduction

Rhizobia and sinorhizobia are beneficial soil bacteria that form symbiotic relationships with leguminous plants. Through a complex process, the bacteria induce the plants to grow root nodules in which the bacteria then reside using plant nutrients while fixing nitrogen for the plants. Once in the root nodules, the sinorhizobia then differentiate into bacteroids, and the genes associated with nitrogen fixation are expressed. This symbiotic relationship is still not clearly understood, and there is considerable interest in the molecular basis of symbiosis[1] and its impact on plant evolution.[2]

Certain strains of sinorhizobia, *Sinorhizobium meliloti* L5–30 in particular, synthesize a class of aminocyclitol compounds called rhizopines. Rhizopines are believed to provide a biased rhizosphere, in which bacteria able to catabolize them are given a selective advantage over those which cannot.[3] This could increase the efficacy of commercial agricultural products called nitrogen inoculants, and thus rhizopines have received attention by those interested in their agricultural and microbiological properties.[4] To date, only two rhizopines have been identified: *scyllo*-inosamine (**1**) and 3-*O*-methyl-*scyllo*-inosamine (**2**).[5]

MosA is a protein found in *S. meliloti* L5–30 and has been implicated in the biosynthesis of the rhizopine **2** from **1**, as indicated in Scheme 1.[5,6] MosA was assigned the function of an *O*-methyltransferase based on indirect evidence, specifically the detection of both **1** and **2** in root nodules infected by bacteria containing the *mos*A gene, while only **1** was detected in the absence of this gene. This assignment has been independently discussed in the literature[7,8] because MosA shares 45% sequence identity to *Escherichia coli* dihydrodipicolinate synthase (DHDPS), an enzyme responsible for the branch point reaction in the biosynthesis of L-lysine and *meso*-diaminopimelate.[9,10] DHDPS catalyzes the condensation of pyruvate with L-aspartate-β-semialdehyde (ASA) to form dihydrodipicolinate (Scheme 1), and the enzyme has been well-studied, particularly in a recent series of structure–function studies by Gerrard and coworkers on the DHDPS from *E. coli*.[11–17] These studies indicate that DHDPS follows a ping-pong mechanism, in which

[a] *Dr. C. P. Phenix, P. H. Tam, Prof. Dr. D. R. J. Palmer*
Department of Chemistry, University of Saskatchewan
110 Science Place, Saskatoon, SK S7N 5C9 (Canada)
E-mail: dave.palmer@usask.ca

[b] *K. Nienaber, P. H. Tam, Prof. Dr. L. T. J. Delbaere, Prof. Dr. D. R. J. Palmer*
Department of Biochemistry, University of Saskatchewan
107 Wiggins Road, Saskatoon, SK S7N 5E5 (Canada)

[c] *Dr. C. P. Phenix*
Present address: TRIUMF, University of British Columbia
4004 Wesbrook Mall, Vancouver, BC V6T 2A3 (Canada)

[d] *P. H. Tam*
Present address: Department of Chemistry, University of Alberta
11227 Saskatchewan Drive, Edmonton, AB T6G 2G2 (Canada)

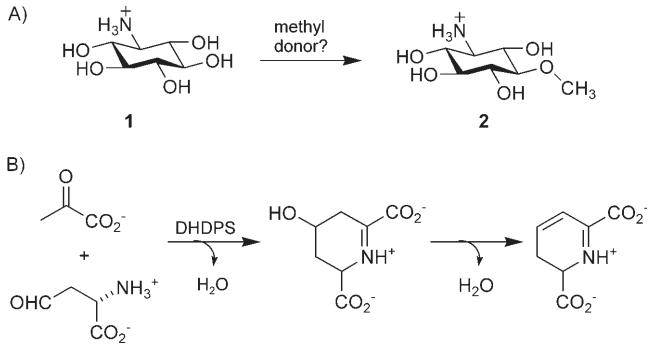

Scheme 1. A) The methyltransferase reaction in rhizopine biosynthesis previously ascribed to MosA. B) The dihydrodipicolinate synthase reaction known to be catalyzed by MosA.

pyruvate Schiff-base formation precedes binding of ASA, and that L-lysine is an allosteric, hyperbolic inhibitor.[14] Sequence alignments indicate that all active-site residues known from studies of DHDPS are conserved in MosA. In fact, our lab has demonstrated that MosA is a DHDPS, with Michaelis constants (0.27 and 0.13 mM for pyruvate and ASA, respectively) similar to other DHDPS enzymes.[18] This finding does not rule out the possibility that MosA is also a methyltransferase, "moonlighting" with a second function. To date, in at least six publications[3–6,19,20] MosA is described as an apparent *O*-methyltransferase. However, no methyl donor has been proposed for the methyl transfer reaction, which bares no resemblance to the Schiff-base-dependent aldolase mechanism catalyzed by DHDPS. As pointed out by Babbitt and Gerlt,[8] there is no precedent for a methyl transfer mechanism involving a protonated Schiff base functioning as an electron sink, although such a mechanism can be drawn with 2-oxobutyrate (Scheme 2). *S*-Adenosylmethionine (SAM) is the only known cosubstrate for *O*-methyl transfer.

Here we report the crystal structure of MosA forming a covalent adduct with pyruvate. We have synthesized **1** and **2** and

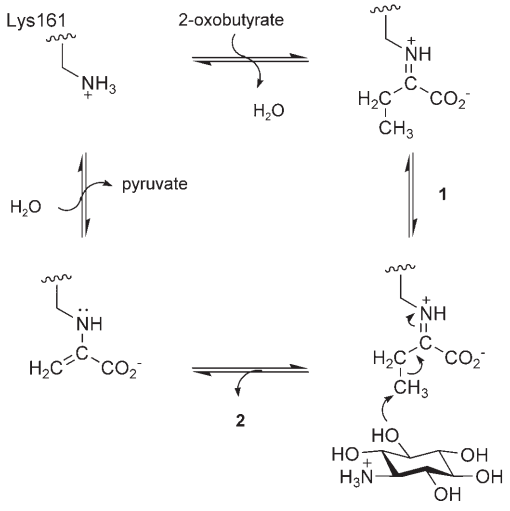

Scheme 2. A postulated, albeit unprecedented, mechanism for 2-oxobutyrate acting as a methyl donor.

used HPLC and isothermal titration calorimetry to look for in vitro MosA-catalyzed methyl transfer, or any apparent interaction of MosA with rhizopines or methyl donors, including the effects of rhizopines on the MosA-catalyzed DHDPS reaction. We also have used isothermal titration calorimetry (ITC) to assess the thermodynamics of Schiff base formation by pyruvate and its four-carbon homologue, 2-oxobutyrate.

Results and Discussion

Rhizopine synthesis

Synthetic methods have been developed for the preparation of aminocyclitols as these compounds are crucial components of many antibiotics[21,22] and potential lead compounds for glycosidase inhibitors,[23] but when we began our work the preparation of **1** had not been reported for 40 years. Early syntheses of **1** suffer from poor yields and the need to separate stereoisomers of the aminocyclitol.[24–26] More recently, a procedure has been published,[27] but excessive steps and the requirement of flash column chromatography for most steps limit its convenience. The lack of a convenient synthesis is somewhat surprising given that **1** is also a precursor of streptomycin.[28,29] The synthesis of **2** has been reported starting from *myo*-inositol in an overall yield of less than 10%.[30]

Generating the *scyllo*-inosamine **1** from inexpensive *myo*-inositol is mainly a matter of isolating the axial 2-position for reaction. We pursued three distinct strategies toward this goal: 1) selective silylation of the 2-hydroxyl group of the 1,3,5-monoorthoformate derivative with *tert*-butyldimethylsilyl chloride in 2,6-lutidine, followed by benzylation of the 4/6-positions and removal of the silyl group; 2) generating the 1,4,5,6-tetra-*O*-benzyl-*myo*-inositol, followed by selective benzylation of the equatorial 3-hydroxyl group via the dibutylstannylene; and 3) perbenzylation of *myo*-inositol followed by selective cleavage of the 2-*O*-benzyl group with $SnCl_4$. In our hands, the third of these strategies, shown in Scheme 3, was most successful.

Starting from the widely used (and commercially available) monoorthoformate of *myo*-inositol **3**, benzylation with NaH in DMF leads to the tribenzyl-orthoformate **4**. Subsequent removal of the orthoformate with Dowex® 50WX8-100 (H^+) ion-exchange resin in methanol and a few drops of dichloromethane provided the tribenzyl inositol; simply filtering off the resin and evaporating the solvent yields inositol derivatives sufficiently pure for further reactions. Benzylation of the tribenzyl inositol in DMF with NaH and BnBr provided the symmetrical hexabenzyl inositol **5** which easily crystallizes from methanol after routine work up. Direct perbenzylation of *myo*-inositol (that is, without first forming the orthoformate) was ineffective in our hands. Regioselective deprotection of the axial benzyl group to give pentabenzyl **6** is achieved by $SnCl_4$ in dry dichloromethane.[31] This results in a mixture of deprotected inositols, although the symmetrical pentabenzyl **6** is obtained in 58% yield. Since unreacted **5** can be recovered from the reaction mixture, subsequent isolation and treatment with $SnCl_4$ results in greater overall efficiency. Routine mesylation in pyridine and S_N2 azidolysis in DMF gives the protected azide **7**

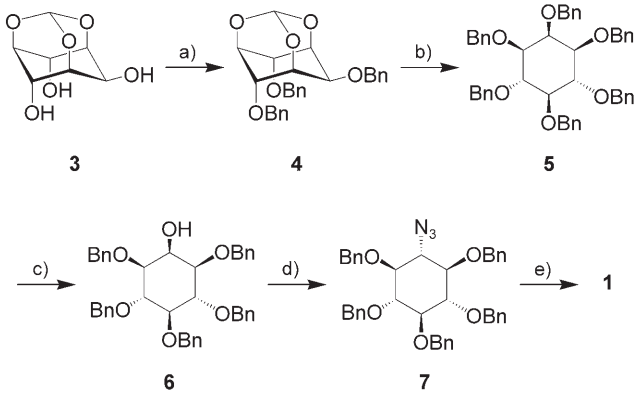

Scheme 3. Reagents and conditions: a) NaH, BnBr, DMF, 92%; b) 1) Dowex (H^+) MeOH, 2) NaH, BnBr, DMF, 94%; c) $SnCl_4$, CH_2Cl_2, 58%; d) 1)mesyl chloride, pyridine, 2) NaN_3, DMF, 80 °C, 63%; e) 1) $tBoc_2O$, H_2, 10% Pd/C, 2) Dowex (H^+), 74%. Bn = benzyl; DMF = *N*,*N*-dimethylformamide; *t*Boc = *tert*-butoxycarbonyl.

possessing the desired *scyllo* stereochemistry with no trace of the *myo*-isomer. Simultaneous reduction of the azide and routine hydrogenolysis proved difficult initially, apparently due to poisoning of the Pd catalyst by the amino group. Fortunately, this problem was solved by the in situ protection of the amine with *t*-Boc_2O, allowing efficient cleavage of the benzyl ether.[32] Once the hydrogenolysis was complete, stirring overnight in the presence of Dowex (H^+) resin followed by loading the suspension into a small column and elution with 0.1 M HCl provided the amine **1** as the HCl salt. In all, **1** was obtained in 25% yield starting from *myo*-inositol with flash column chromatography required for only two steps.

A strength of the route described above is that it lends itself to modular changes. In this case, **2** was prepared as outlined in Scheme 4 by introduction of the methyl group prior to benzylation. The orthoformate **3** was reacted with 1.1 equiv of CH_3I and NaH and allowed to stir for 12 h, after which reaction with 2.2 equivalents of NaH and benzyl bromide gave **8** in 75% yield. Hydrolysis with Dowex (H^+) and perbenzylation gave the methyl ether **9** and upon treatment with $SnCl_4$ yield-

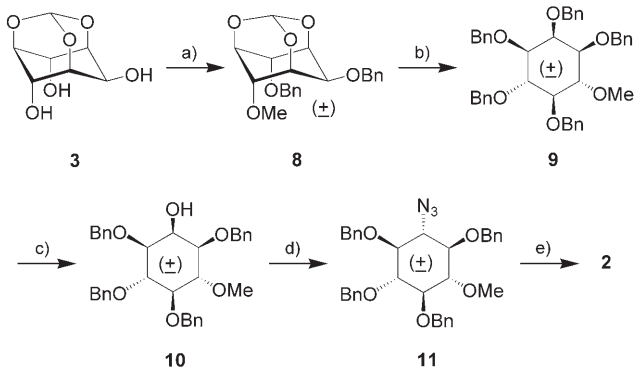

Scheme 4. Reagents and conditions: a) 1) NaH, CH_3I, DMF, 2) NaH, BnBr, 75%; b) 1) Dowex (H^+), MeOH, 2) NaH, BnBr, DMF, 95%; c) $SnCl_4$, CH_2Cl_2, 58%; d) 1) mesyl chloride, pyridine, 2) NaN_3, DMF, 80 °C, 62%; e) 1) $tBoc_2O$, H_2, 10% Pd/C, 2) Dowex (H^+), 79%.

ed alcohol **10**. Mesylation and azidolysis gave racemic **11**. Subsequent simultaneous deprotection and azide reduction produced the racemic amine **2** in overall 20% yield with silica gel chromatography only required for three steps. This route is similar in its approach to that of Kreif et al.[30] but proceeds in more than double their reported yield.

Protein crystallography

The MosA structure was solved using AMoRe from the CCP4 suite of programs[33] with DHDPS from *E. coli* (1DHP)[9] as a starting model. Refinement was carried out with REFMAC5 and model building with Coot, both from the CCP4 suite. Even though L-lysine was present in the crystallization solution, no free lysine was evident in the structure. We do not interpret the absence of L-lysine from the structure as an indication that the enzyme lacks a lysine-binding site; indeed, we have observed that it inhibits the MosA-catalyzed DHDPS reaction.[18] The resulting 1.95 Å data had a merging *R* value of 0.10 with unit cell values consistent with previous unpublished data. Final R_{work} was 0.20 with R_{free} of 0.26. Final model checking was carried out with PROCHECK[34] showing 91% in most favored regions, 7.8% in favored regions, 0.4% in generously allowed regions, and 0.8% in disallowed regions due to Tyr106, which is twisted into the adjacent subunit as has been previously described,[9] and Asp265, which is found in an external loop of the C-terminal domain. Further refinement statistics can be found in Table 1. The asymmetric unit of MosA crystals contains a homodimer; a crystallographic twofold axis generates the molecular tetramer.

Gel filtration chromatography indicated that MosA was tetrameric in solution at concentrations used for the analyses. The refined structure showed that the enzyme crystallized as a tetramer, as shown in Figure 1, consistent with DHDPS from other bacteria. The tetrameric structure has been shown to be an important aspect of reactivity with engineered dimeric forms showing low activity, although it is not yet clear why this is so.[35] Each monomer displays the canonical $(\beta/\alpha)_8$ ("TIM") barrel fold, with only a few additional features. Comparison of the structures of monomers of MosA and *E. coli* DHDPS using DaliLite[36] indicated a root-mean-square deviation of 1.0 Å, using both an unliganded structure, pdb-designated 1DHP,[9] and a lysine-bound structure, 1YXD.[13]

The active site of DHDPS from *E. coli* contains a set of highly conserved residues believed to be required for catalysis. Results from X-ray crystallography and site-directed mutagenesis experiments[9,11,13,15] are consistent with Lys161 acting as the nucleophile that forms a Schiff base with pyruvate. Tyr133, Thr44, and Tyr107′ of the *E. coli* enzyme appear to form a catalytic triad that may act as a proton shuttle (in which Tyr107′ is from an adjacent subunit). Arg138 is positioned at the mouth of the active site, and appears to be involved in binding of the second substrate, ASA, in the ping-pong mechanism. The active site of DHDPS is found at the C-terminal "face" of the barrel, typical of TIM barrel enzymes.

The active site of MosA contains all the features of other DHDPS enzymes, some of which are indicated in Figure 2.

Table 1. Final data collection and refinement statistics for MosA using REFMAC5 from the CCP4 suite of programs.[27] Numbers in parentheses refer to highest resolution shell.

Data collection	
space group	$C222_1$
unit cell dimensions	
a [Å]	68.9
b [Å]	138.7
c [Å]	123.2
no. molecules in asymm. unit	2
resolution range [Å]	19.75–1.95 (2.00–1.95)
no. reflections measured	254154
no. unique reflections	41799 (4563)
R_{sym}	0.10 (0.26)
completeness [%]	93.4 (74.4)
redundancy	3.3 (2.5)
mean $I/\sigma(I)$	8.48 (3.94)
Refinement statistics	
resolution range [Å]	10.50–1.95 (2.00–1.95)
R_{work} (37312 reflections)	0.198 (0.32)
R_{free} (2073 reflections)	0.264 (0.44)
R_{cryst} (39385 reflections)	0.201
no. non-H protein atoms	4408
no. water molecules	322
mean B factors [Å^2]	
main-chain atoms	19.6
side-chain atoms	22.4
water molecules	24.2
SO_4^{2-} atoms	31.7
r.m.s. deviations from ideal geometry	
bond distances [Å]	0.018
bond angles [°]	2.65
dihedral angles [°]	18.6
improper angles [°]	0.20
Ramachandran statistics	
most favored [%]	91.0 (431 a.a.)
favored [%]	7.8 (39 a.a.)
additional allowed [%]	0.4 (2 a.a.)
disallowed [%]	0.8 (4 a.a.)

$R_{sym} = \Sigma|\langle I_{hkl}\rangle - I_{hkl}|/|I_{hkl}|$, where $\langle I_{hkl}\rangle$ is the average intensity over symmetry-related reflections and I_{hkl} is the observed intensity. $R_{value} = \Sigma||F_o| - |F_c||/\Sigma|F_o|$, where F_o and F_c are the observed and calculated structure factors. For R_{free} the sum is done on the test set reflections (5% of total reflections), for R_{work} on the remaining reflections, and for R_{cryst} on all reflections included in the resolution range. *Note*. 40% of reflections in the outer shell had $I/\sigma(I) > 3$. Of the 4 amino acids in disallowed Ramachandran space, two are the Tyr106 residues that stretch into the other monomer active site; the analogoues Tyr residue is found in a strained conformation in other DHDPS structures (see text). The other two are Asp265 residues that are located on an external loop, with average B factors of 29 Å^2 for the non-hydrogen atoms.

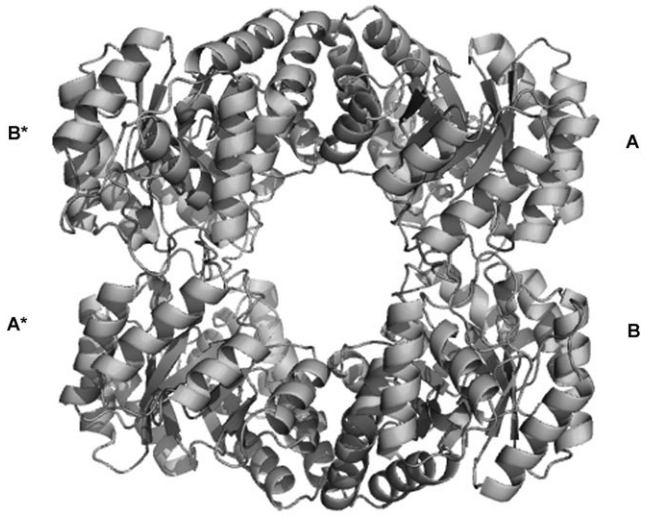

Figure 1. Tetramer of MosA. The asymmetric unit found in the crystal structure contains a dimer. Image generated with PyMol (Palo Alto, CA).

Note that there is only a small difference in numbering between the *E. coli* DHDPS and MosA. Lys161 of MosA is found at the C-terminal end of β-strand 6 of the barrel, forming an imine or enamine adduct with pyruvate, the first substrate in the ping-pong mechanism of the DHDPS reaction. As indicated in Figure 2B, the density seen is clearly consistent with a pyruvate adduct. Adjacent to this residue, located at the end of strand 5, is Tyr132. The hydroxyl group of this residue appears poised to act as an acid/base catalyst in the Schiff base formation reaction between Lys161 and pyruvate, with the phenolic oxygen just 3.35 Å from the imine carbon atom. A small helical extension from strand 2 of MosA contains a threonine–threonine dyad, Thr43 and Thr44. The side-chain oxygen of Thr43 is 4.36 Å from the side-chain oxygen of Tyr132, and is proposed to form the proton relay through hydrogen bonding to the phenolic oxygen of Tyr106′, just 2.82 Å away. The Tyr106′ side chain reaches into the active site of MosA from a loop extending from strand 4 of the adjacent subunit. Arg137 is found at the mouth of the active site, on a helical projection from strand 5. Gly186 at the C terminus of strand 7, has been proposed to provide a favorable dipole for the binding and reaction of the hydrate of ASA. At the end of strand 8, Ile203 appears to delimit the volume adjacent to the lysine–pyruvate adduct, which may contribute to the selectivity of the enzyme toward pyruvate. The close correspondence of the MosA active site to that of *E. coli* DHDPS is shown in Figure 2C. The mechanism for the MosA-catalyzed DHDPS reaction can therefore be proposed to proceed as in Scheme 5, in simile with the DHDPS mechanism put forth by Gerrard and coworkers.[11]

2-Oxobutyrate interacts with MosA

We have already demonstrated that MosA can function as a DHDPS in vitro and in vivo.[18] With the two rhizopines in hand, we were able to investigate the two postulated mechanisms of methyl transfer: with SAM or 2-oxobutyrate as a methyl donor. Of these, the SAM mechanism seemed more plausible, since there is ample precedent of such reactions, despite the lack of any apparent SAM-binding motif in MosA. However, interaction of 2-oxobutyrate with MosA was also reasonable, since most pyruvate-utilizing enzymes will also utilize 2-oxobutyrate. We have found MosA to behave very much like the *E. coli* DHDPS with respect to catalysis and inhibition by lysine,[18] but there is some conflict in the literature regarding the effect of 2-oxobutyrate on DHDPS. A review article from 1996 states categorically that the *E. coli* enzyme is not inhibited by pyruvate ana-

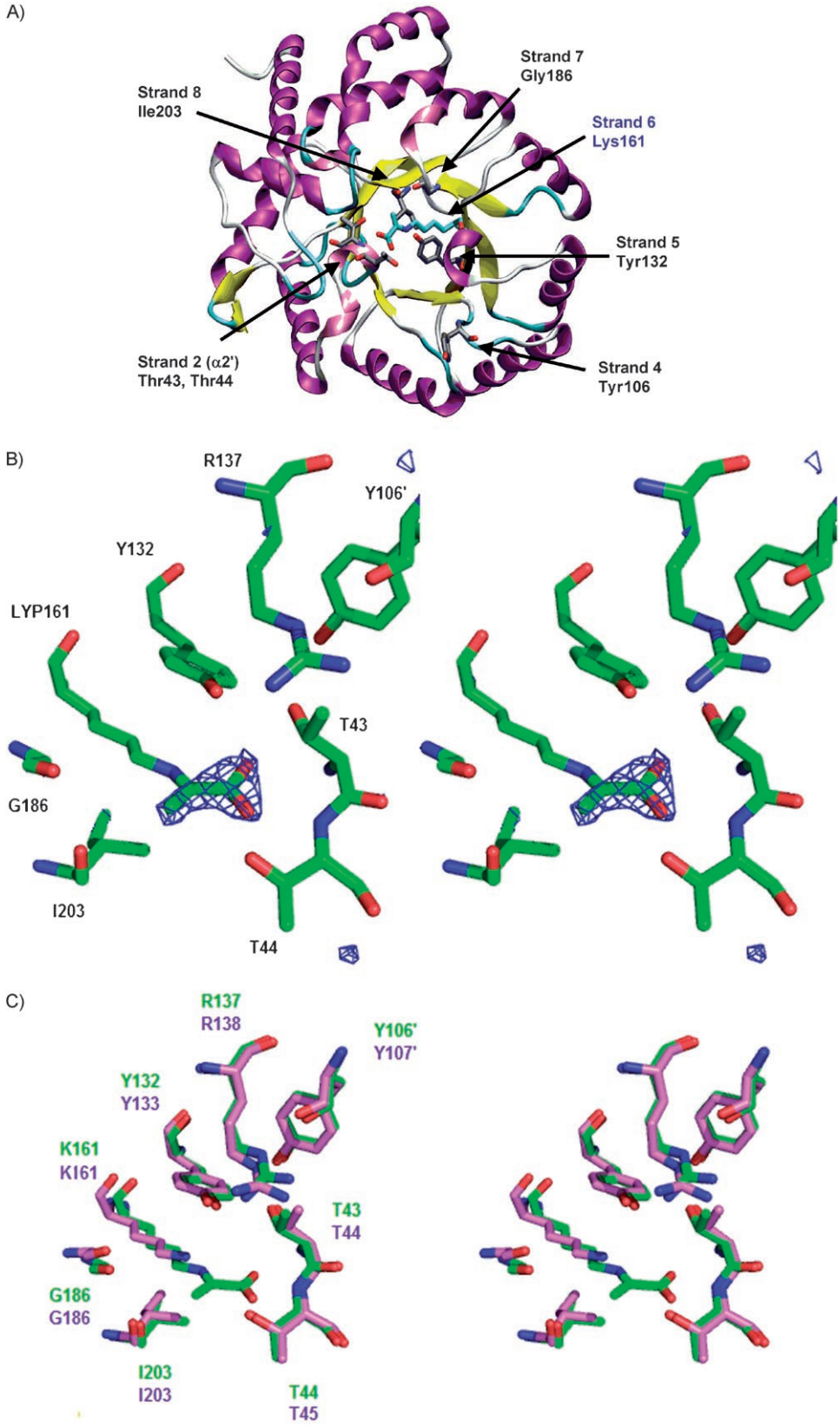

Figure 2. The active site of MosA. A) The monomer, with active-site residues labelled. The adduct of Lys161 is highlighted using cyan for the carbon atoms. Image generated with VMD (Urbana, IL) followed by POV-Ray (Victoria, Australia). B) Stereoview difference map ("omit map", F_o-F_c contoured to 3σ) indicating the electron density due to pyruvate modification of Lys161. Image generated with PyMol. C) Stereoview superposition of the active-site residues of MosA with DHDPS from *E. coli*. Carbon atoms of MosA are indicated in green; DHDPS carbon atoms in mauve. Structural alignment was performed with DaliLite.[36] Image generated with PyMol.

logues such as 2-oxobutyrate,[37] but in 1997 Karsten[38] reported competitive inhibition of *E. coli* DHDPS by 2-oxobutyrate, with $K_i = 0.83$ mM.

We find 2-oxobutyrate to be a competitive inhibitor of MosA with respect to pyruvate. The inhibition constant, $K_i = 0.9 \pm 0.3$ mM, was evaluated by Dixon plot, which clearly fit the model for competitive inhibition,[39] as shown in Figure 3. Furthermore, the presumed Schiff-base intermediate formed by 2-oxobutyrate could be trapped by treatment with sodium borohydride. We previously showed that treatment of MosA with sodium borohydride in the presence of pyruvate resulted in an inactivated enzyme which was increased in molecular weight by an amount corresponding to the reduced pyruvate adduct, whereas treatment with sodium borohydride alone did not affect activity.[18] Similarly, treatment of MosA in the presence of 2-oxobutyrate resulted in an inactivated enzyme whose activity could not be restored upon dialysis. Treatment of MosA with $NaBH_4$ followed by HPLC-MS resulted in a peak corresponding to a mass of 33342 $[M+H]^+$, the mass expected for MosA without any modifications, demonstrating that the reagent itself does not affect the mass of the protein. Treatment of MosA with $NaBH_4$ in the presence of 2-oxobutyrate resulted in a peak corresponding to a mass of 33427 $[M+H]^+$. The difference in the masses is 85, corresponding to the mass difference expected for a reduced Schiff base adduct of MosA with 2-oxobutyrate. Despite acting as a pyruvate analogue in the active site of MosA, we observed no evidence that 2-oxobutyrate could react with aspartate semialdehyde to form a methyldihydrodipicolinate; this suggests that the steric demand of the additional carbon atom does not

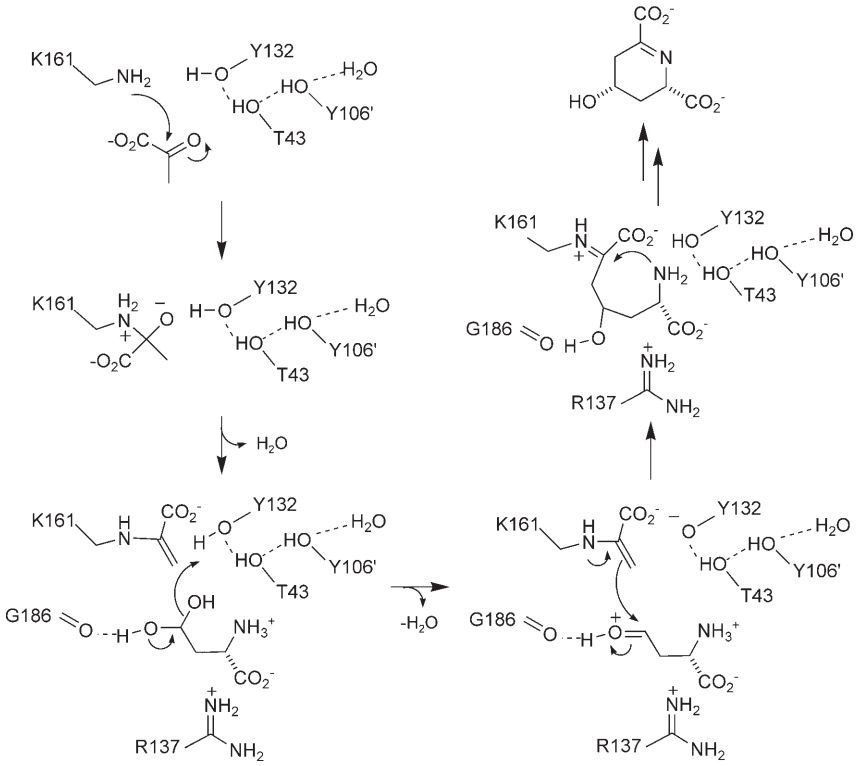

Scheme 5. Proposed mechanism of the MosA-catalyzed DHDPS reaction, adapted from Dobson et al.[11]

permit the aldolase reaction. This was also observed for *E. coli* DHDPS.[40]

HPLC was used to assess methyl transfer from 2-oxobutyrate to **1**. Although pyruvate is a product of the postulated reaction of Scheme 2, a coupled assay with lactate dehydrogenase and NADH is not possible because 2-oxobutyrate is also a substrate of lactate dehydrogenase. Derivatization of the rhizopines with 9-fluorenylmethyloxycarbonyl chloride (FMOC-Cl) following a procedure reported for glucosamine[41] resulted in adducts that could be separated by reversed-phase HPLC. Reaction mixtures of MosA, 2-oxobutyrate and **1** were prepared in phosphate buffer at pH 7.0, since these conditions minimized the hydrolysis of FMOC-Cl, but MosA retained (DHDPS) activity. However, formation of the FMOC derivative of **2** could not be detected under these conditions.

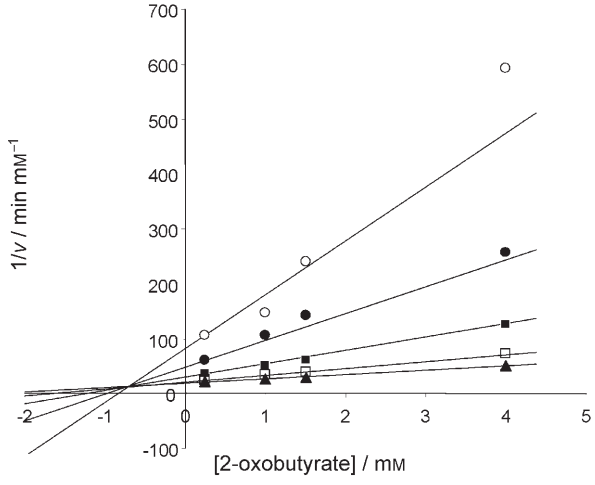

Figure 3. Dixon plot indicating competitive inhibition by 2-oxobutyrate with respect to pyruvate of the MosA-catalyzed DHDPS reaction. Reactions performed in 100 mM imidazole, 10 mM K_2HPO_4, pH 7.7, at 37 °C. Pyruvate concentrations: 0.125 (○), 0.25 (●), 0.5 (■), 1.0 (□), and 1.5 mM (▲).

Investigation of SAM as a methyl donor

As stated above, *O*-methyltransferases typically rely on SAM as a methyl donor. We monitored a reaction mixture of **1** and SAM in the presence of MosA. To do so, an HPLC assay was developed to observe the disappearance of SAM and the appearance of the product *S*-adenosylhomocysteine (SAH). Commercially available SAM comes only 70% pure, and unfortunately, one of the major contaminants is SAH. Consequently, any HPLC assays that measured the decrease in amounts in SAM and increased amounts of SAH must take this into account. Reaction mixtures containing MosA, SAM and **1** were incubated at 37 °C for 3 h, after which protein was removed by ultrafiltration and aliquots injected into the HPLC. SAM and SAH were detected at 260 nm using retention times that were determined by the commercial standards. Methyltransferase activity was qualitatively diagnosed by comparing the ratios of the areas of SAM to SAH. However, no change in the ratio of peak areas could be detected; in the presence and absence of MosA, the ratio of SAM to SAH was 27:1. The same assay was used to detect methyl transfer from SAM to catechuic acid catalyzed by catechol *O*-methyltransferase (COMT), as shown in Figure 4. After incubation of COMT with catechuic acid and SAM, the appearance of SAH could clearly be detected, as indicated by a SAM/SAH ratio of 10:1, validating the method.

Rhizopines do not inhibit DHDPS activity

If MosA is involved in rhizopine synthesis, then the protein must interact with the putative substrates in some way. The first attempt to observe such an interaction was an investigation of rhizopines **1** and **2** on the MosA-catalyzed DHDPS reaction. If the rhizopines bind at the same active site used for the aldolase reaction then some effect on the rate would be expected. No such effects were observed after pre-incubation of MosA with up to 10 mM rhizopines, in contrast to the measurable effects of 2-oxobutyrate described above.

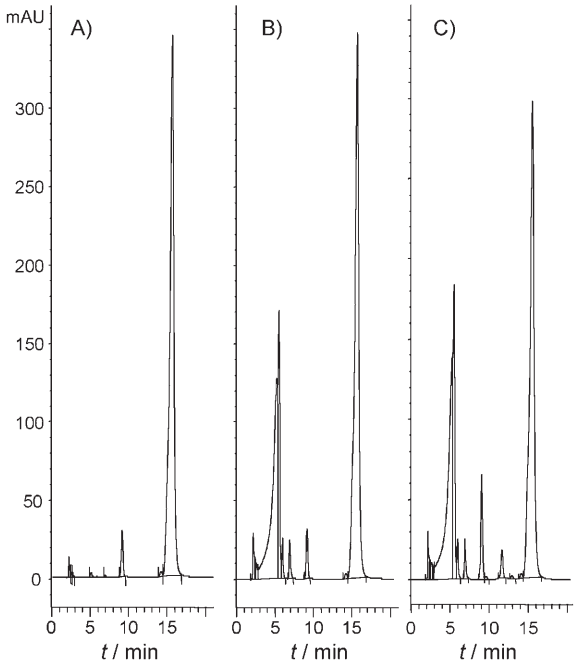

Figure 4. Reverse-phase HPLC chromatograms of methyl transfer assays. Retention times: SAH, 9.2 min; SAM, 15.7 min; A) commercially available SAM (2.5 mM) in imidazole buffer (100 mM imidazole, 10 mM K_2HPO_4, pH 7.6). B) **1** (2.5 mM), SAM (2.5 mM) and MosA (0.23 μM) incubated for 3 h at 37 °C in imidazole buffer (100 mM imidazole, 10 mM K_2HPO_4, pH 7.6). C) Methyl transfer from SAM to catechuic acid catalyzed by COMT in phosphate buffer (200 mM NaH_2PO_4, 5 mM $MgCl_2$, pH 7.4), 100 units COMT, 3 mM SAM and 2 mM catechuic acid 2.5 h, 37 °C.

Isothermal titration calorimetry (ITC)

ITC using a microcalorimeter directly measures the heat released or absorbed by the stepwise titration of one reactant into a sample cell containing the other, and can therefore be used to measure covalent and noncovalent molecular interactions. In principle, one can determine in a single experiment the affinity (K_a), enthalpy (ΔH) and stoichiometry (n) of a binding event, subsequently allowing the calculation of Gibbs free energy (ΔG) and entropy (ΔS) of association. ITC has contributed to a greater understanding of binding affinity especially in protein–protein and protein–small molecule interactions.[42] Due to its versatility in studying various systems of low and high affinity, ITC is expected to play a vital role in rational drug design and the study of protein–protein interactions.[43] Furthermore, since ITC is uniquely able to quantify enthalpic and entropic contributions, it is a useful bridge between computational and experimental techniques.[44]

We titrated MosA with a known substrate, pyruvate, and it's analogue, 2-oxobutyrate, as well as SAM, **1**, and **2**. Schiff-base formation between enzyme and substrate is very likely a reversible, low-affinity system. Criteria for appropriate analysis of low-affinity systems have been set out by Turnbull and Daranas.[45] If the stoichiometry of binding is known, the concentrations of the two binding components are known with accuracy, there is a sufficient signal-to-noise ratio, and a large enough portion of the binding isotherm is used, then reliable data can be extracted. For pyruvate, an injection interval of 200 seconds was sufficient to allow equilibrium to be re-established. The resulting hyberbolic isotherm is shown in Figure 5. The K_d extracted for pyruvate's interaction with MosA was 0.4 mM; the kinetically-determined K_m with respect to pyruvate reported for MosA[18] and for DHDPS from *E. coli*[14] are between

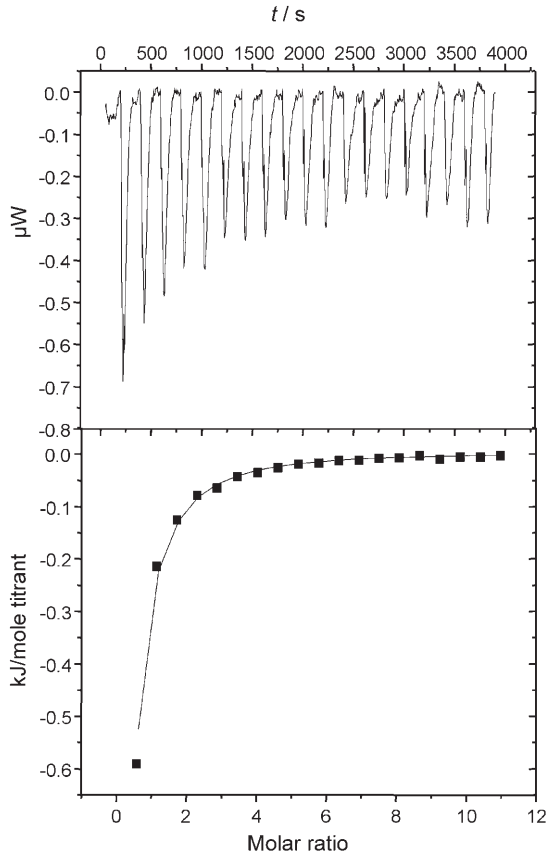

Figure 5. ITC titrations of pyruvate into buffered MosA solutions. Top graph shows the raw data for 19 injections (5 μL) of pyruvate (50 mM) into an imidazole buffered MosA solution (0.07 mM based on monomer molar mass) at 15 °C. The bottom graph shows data points as energy (as kJ mol^{-1} titrant) as a function of molar ratio with the solid line representing the fit to the 1:1 binding model from Bindworks 1.0 (Calorimetry Sciences Corp., Lindon Utah).

0.2 and 0.3 mM. This similarity lends support to the assertion of Turnbull and Daranas that low-affinity systems can be studied effectively by ITC when the appropriate criteria are met.

The thermodynamic values obtained for Schiff base formation between MosA and pyruvate, summarized in Table 2, indicate that the process is entropically driven. This can be accounted for by the burial of the negatively charged pyruvate into the active site of MosA, which will release water from both the surface of pyruvate and the MosA active site with increased entropy. Furthermore, since the reaction itself involves MosA and pyruvate forming the MosA–pyruvate Schiff base and water, no large decrease in rotational and translational entropy is expected. The enthalpy term of this reaction is negative, likely because of the formation of the imine along with fa-

Table 2. Thermodynamic data determined by ITC.[a]

Ligand	T [°C]	K_d [mM]	ΔH [kJ mol^{-1}]	ΔG [kJ mol^{-1}]	$T\Delta S$ [kJ mol^{-1}]
pyruvate	25	0.4 ± 0.1	-3.8 ± 0.6	-19.8 ± 0.5	16 ± 1
pyruvate	15	0.5 ± 0.1	-3.7 ± 0.1	-19.1 ± 0.5	16 ± 1
2-oxobutyrate	25	2 ± 1	-3 ± 2	-15 ± 2	12 ± 3

[a] Experiments performed in imidazole buffer (100 mM, pH 7.7). Values are an average of at least two independent trials ± standard deviation.

vorable interactions in the active site of MosA. The observed enthalpy change is small, and therefore subject to greater influence of experimental uncertainty, such as protein concentration, although our results were consistent. Similar thermodynamic values were obtained by ITC for rho protein, an RNA-binding transcription terminator factor, covalently binding an inhibitor through a Schiff base formed between a binding-site lysine and an aldehyde group.[46] We repeated our experiments at two different temperatures, 25 and 15 °C, and the results are within experimental error of one another; this suggests that no large heat capacity change is associated with this interaction. This is consistent with the lack of an apparent conformational change upon pyruvate binding. We sought to compare our thermodynamic values with similar enzymes, such as aldolases or other Schiff-base-forming enzymes, but could find no values with which to compare. The previously mentioned experiments with rho protein and a man-made inhibitor are the only precedent. This is the first reported example of an enzyme–covalent reaction intermediate which has been thermodynamically characterized by ITC.

Titration with 2-oxobutyrate in place of pyruvate gave very similar results, although the increase in entropy is smaller, consistent with the proposal that this molecule behaves as a pyruvate analogue. The value of the dissociation constant is similar to the observed K_i value.

In contrast, we saw no difference between titration of rhizopine into a solution of MosA and a titration of rhizopine into buffer alone. This was also true for a titration of **1** into a 2-oxobutyrate-saturated solution of MosA. This indicates that there is no significant binding event occurring between MosA and rhizopines. Titration of MosA with SAM also indicated no protein–ligand binding.

Conclusions

The high-resolution structure reported here supports all other evidence that MosA is a DHDPS. The lysine–pyruvate adduct observed at the active site of the enzyme is consistent with the assignment of Lys161 as the key residue in the Schiff-base mechanism. Other key residues identified in the DHDPS from *E. coli* are also present in MosA, including the proposed catalytic triad Tyr132, Thr43, and Tyr106′, and Arg137 at the mouth of the active site. The quaternary structure, known to be important for activity of the *E. coli* enzyme, is maintained in MosA. In the presence of pyruvate, a crystal of the enzyme liganded by L-lysine could not be attained. It is noteworthy that no DHDPS structure containing both substrate and allosteric inhibitor has been obtained despite our efforts and those of other groups, perhaps indicating that this complex is inherently unwilling to crystallize. MosA is competitively inhibited by 2-oxobutyrate and can be inactivated by reduction of the active-site imine formed. Isothermal titration calorimetry shows that the covalent binding of pyruvate and of 2-oxobutyrate to MosA proceed with a significant increase in entropy and a small decrease in enthalpy in both cases.

We found no in vitro evidence for the interaction of MosA with rhizopines **1** or **2**. We saw no methyl transfer from 2-oxobutyrate or from SAM, and the rate of the MosA-catalyzed DHDPS reaction was not affected by rhizopines. ITC could not detect MosA-rhizopine binding. This result does not suggest that the rhizopine concept itself is flawed, and compounds **1** and **2** may yet be exploited agriculturally in the promotion of beneficial plant-microbe interactions.

Experimental Section

Organic synthesis: Chemical reagents for organic synthesis, chromatography, biochemistry and molecular biology, including fine chemicals, buffers, salts, and media, were obtained from Sigma–Aldrich or VWR CanLab (Mississauga, ON), and were categorized as Molecular Biology Grade or were the highest grade available. Pall Life Science Nanosep centrifugal devices were purchased from VWR Canlab. Aspartate-β-semialdehyde was synthesized following the method of Morris.[47] Syntheses that required anhydrous conditions were performed under an inert atmosphere of dried argon or nitrogen. Glassware was dried overnight in an oven set at 120 °C and assembled under a stream of inert gas. Dichloromethane was freshly distilled from calcium hydride. Thin-layer chromatography was performed on precoated silica gel plates (Merck Kieselgel $60F_{254}$, 0.25 mm thickness) and visualized with phosphomolybdic acid reagent, iodine vapors, ninhydrin (1.5% w/v solution in *tert*-butanol) or ultraviolet light at 254 nm. Flash chromatography was performed with Merck silica gel 60 (230–400 mesh). NMR spectra were obtained on a Bruker 500 MHz spectrometer. Chemical shift was reported in ppm downfield from tetramethylsilane, with the solvent signal as reference. Infrared spectra were obtained on a Bioread FTS-40 Fourier transform interferometer using a diffuse reflectance cell (DRIFT); diagnostically important signals are reported in ν (cm^{-1}). Mass spectrometric characterization of organic compounds was performed on an API Qstar XL pulsar hybrid LC/MS/MS. Melting points were measured on a Gallencamp melting point apparatus and were not corrected. NMR, mass spectrometry and elemental analysis facilities are a part of the Saskatchewan Structural Sciences Centre. Protein mass spectrometry was performed at the Saskatoon Cancer Centre.

*2,4,6-Tri-O-benzyl-1,3,5-O-methylidyne-myo-inositol (**4**)*.[48] To a solution of **3** (1.0 g, 5.2 mmol) in dry DMF (40 mL) at room temperature and under argon, sodium hydride (1.25 g of 60% dispersion in oil, 31.2 mmol; ***CAUTION!*** evolution of hydrogen gas) was added. The reaction mixture was stirred for 10 min and then benzyl bromide (3.7 mL, 31 mmol) was added dropwise followed by continuous stirring for an additional 14 h. The reaction was quenched with water (1 mL) and then partitioned between dichloromethane (200 mL) and water (100 mL). The organic phase was dried ($MgSO_4$) and evaporated in vacuo leaving an oil that was crystallized (ethyl acetate/hexane 10:1) to give **4** (2.2 g, 4.8 mmol, 92% yield). ^{1}H NMR (500 MHz, $CDCl_3$): $\delta = 4.04$ (m, 1H), 4.30 (m, 2H), 4.35 (m,

2H), 4.43 (m, 1H), 4.55 (m, 6H), 5.52 (d, 0.9 Hz, 1H), 7.31–7.34 (m, 15H).

1,2,3,4,5,6-Hexa-O-benzyl-myo-inositol (**5**).[31] Dichloromethane (1 mL) was added to dissolve the benzyl derivative **4** (0.76 g, 1.7 mmol) at room temperature. The solution was diluted with methanol (15 mL) and Dowex 50W-X8–100 (H^+ form, 3.5 g) was added. The suspension was stirred for 14 h after which TLC confirmed completion of the reaction. The resin was removed by filtering the suspension, and the resulting filtrate was evaporated to yield a white solid. The solid was dissolved in dichloromethane and evaporated three times to ensure sufficient removal of the methanol. Without further purification, the crude product was dissolved in dry DMF (20 mL) and sodium hydride (0.28 g of 60% dispersion in oil, 7 mmol; ***CAUTION!*** evolution of hydrogen gas) was added. The reaction was stirred for five minutes, after which benzyl bromide (0.9 mL, 7 mmol) was added dropwise; the resulting solution was stirred continuously for 14 h. The reaction was quenched with methanol (1 mL) and the solvents removed in vacuo to yield an oil that was dissolved in dichloromethane (50 mL) and extracted with water (50 mL). The organic layer was then dried ($MgSO_4$) and evaporated to yield the crude **5** that was easily purified by crystallization from boiling methanol (1.12 g, 1.6 mmol, 94% yield). ^{1}H NMR (500 MHz, $CDCl_3$): $\delta = 3.38$ (dd, $J = 2.16$, 9.83 Hz, 2H), 3.50 (t, $J = 9.25$ Hz, 1H), 4.06 (m, 1H), 4.11 (t, $J = 9.54$ Hz, 2H), 4.59–4.69 (m, 4H), 4.84–4.95 (m, 8H), 7.28–7.31 (m, 30H).

1,3,4,5,6-Penta-O-benzyl-myo-inositol (**6**). To a solution of **5** (0.10 g, 0.13 mmol) in dry dichloromethane under argon gas, $SnCl_4$ (0.13 mL of a 1 M solution in dichloromethane, 0.13 mmol) was added and the reaction stirred for one hour at room temperature. The reaction was diluted with dichloromethane (2 mL) then quenched with cold water (1 mL). A white precipitate formed that dissolved upon successive washes with brine (3×1 mL). The organic layer was dried ($MgSO_4$) and evaporated to yield a crude oil that was purified by flash chromatography (silica gel, EtOAc/toluene 1:7, *v/v*) to give pure **6** (0.048 g, 0.076 mmol, 58% yield) as a white solid. mp 124–125 °C; ^{1}H NMR (500 MHz, $CDCl_3$): $\delta = 3.41$ (dd, $J =$ 2.7, 9.7 Hz, 2H), 3.47 (t, $J = 9.4$ Hz, 1H), 4.01 (t, $J = 9.5$ Hz, 2H), 4.28 (t, $J = 2.6$ Hz, 1H), 4.75 (s, 4H), 4.85–4.93 (m, 6H), 7.28–7.37 (m, 25H).

1,3,4,5,6-Penta-O-benzyl-2-azido-2-deoxy-scyllo-inositol (**7**).[27] The pentabenzyl inositol **6** (2.6 g, 4.0 mmol) was dissolved in anhydrous pyridine (25 mL). The solution was cooled to 0 °C, and mesyl chloride (1.5 mL, 20 mmol) was added dropwise while stirring. The reaction was allowed to gradually reach room temperature and was stirred for 16 h. The solvents were removed in vacuo to yield a yellow residue that was taken up in CH_2Cl_2 (50 mL), washed with HCl (1 M, 3×50 mL), $NaHCO_3$ (1 M, 2×30 mL), brine (2×30 mL) and dried ($MgSO_4$). Without further purification, the crude mesyl inositol was dissolved in dimethylformamide (22 mL) under argon. Sodium azide (1.25 g, 19.3 mmol) was added in one portion and the reaction kept at a temperature of 80 °C with continuous stirring for 20 h. The mixture was allowed to cool and was then extracted between CH_2Cl_2 (100 mL) and water (100 mL). The organic layer was washed with $NaHCO_3$ (1 M, 1×50 mL), water (1×50 mL), brine (1×50 mL), dried ($MgSO_4$) and evaporated to yield a crude solid. Purification was achieved through flash chromatography (silica gel, ethyl acetate/hexane 1:3 (*v/v*)) yielding azide **7** (1.6 g, 2.5 mmol, 63% yield). mp 95–96 °C; ^{1}H NMR (500 MHz, $CDCl_3$): $\delta =$ 3.44 (t, $J = 9.3$ Hz, 2H), 3.56–3.69 (m, 4H)), 4.94–4.99 (m, 10H), 7.33–7.46 (m, 25H); ^{13}C NMR (127.5 MHz, $CDCl_3$): $\delta = 67.45$, 76.41, 76.44, 76.48, 81.56, 83.03, 83.74, 128.20, 128.25, 128.32, 128.42, 128.70, 128.92, 128.96, 138.27, 138.72, 138.74; IR $\nu_{N3} = 2109$ cm^{-1}.

scyllo-*Inosamine* (**1**). The azide **7** (0.070 g, 0.10 mmol) was dissolved in dichloromethane (1 mL) and diluted with methanol (10 mL). Di-*tert*-butyl dicarbonate (0.24 g, 1.1 mmol) and palladium on activated charcoal (10% *w/w*, 0.14 g) were added. The flask was fitted with a rubber septum and its content was subjected to three rounds of evacuation with a water aspirator followed by flushing with hydrogen gas from a balloon fitted onto a stopcock. The mixture was allowed to react for two days recharging the balloon with fresh hydrogen each day. After this time, the mixture was filtered through a pad of celite, and the solvent was removed in vacuo to yield a white solid. The precipitate was dissolved in water (2 mL) and stirred with Dowex 50WX8–100 (H^+ form, 0.3 g) for 16 h. The mixture was then poured into a 20 mL burette plugged with glass wool forming a column of Dowex. After the Dowex settled into the column the reaction water was allowed to elute and the column washed with another portion of water (10 mL). The amine was eluted with HCl (15 mL, 0.1 M) and isolated as the HCl salt (0.017 g, 0.074 mmol, 74% yield) upon removal of the solvent. ^{1}H NMR (500 MHz, D_2O): $\delta = 3.02$ (t, $J = 10.6$ Hz, 1H), 3.27 (m, 1H), 3.34 (t, $J = 9.2$ Hz, 2H), 3.46 (t, $J = 9.9$ Hz, 2H); ^{13}C (127.5 MHz, D_2O) $\delta = 56.25$, 70.33, 73.57, 74.69; HREIMS: *m/z* calcd for $C_7H_{15}NO_5$ 180.0872 $[M+H]^+$, found 180.0873.

(±)-2,6-Di-O-benzyl-4-O-methyl-1,3,5-O-methylidyne-myo-inositol (**8**). To a solution of **3** (2.0 g, 10 mmol) in dry DMF (60 mL) at room temperature and under argon was added sodium hydride (0.42 g of a 60% dispersion in oil, 10.5 mmol; ***CAUTION!*** evolution of hydrogen gas). The reaction mixture was stirred for 10 min and then iodomethane (0.65 mL, 11 mmol) was added followed by continuous stirring for an additional 14 h. A yellowish clear solution resulted, into which another portion of sodium hydride was added (0.84 g of a 60% dispersion in oil, 21 mmol; ***CAUTION!*** evolution of hydrogen gas) and allowed to react for 10 min. Benzyl bromide (2.5 mL, 21 mmol) was added dropwise, and the reaction was stirred for another 14 h. Water (1 mL) was used to quench the reaction, and the solution was then evaporated to dryness in vacuo at 65 °C, leaving a yellow precipitate which was dissolved in dichloromethane (20 mL), washed with water (20 mL), brine (20 mL) and dried ($MgSO_4$). The organic phase was evaporated to give a yellow oil that was purified by flash chromatography (silica gel, EtOAc/toluene 1:6, *v/v*) yielding **17** (2.9 g, 7.5 mmol, 75% yield) as a colourless oil. ^{1}H NMR (500 MHz, $CDCl_3$): $\delta = 3.41$ (s, 3H), 3.99 (m, 1H), 4.18 (m, 1H), 4.25–4.26 (m, 1H), 4.33–4.34 (m, 1H), 4.38 (m, 1H), 4.46 (m, 1H), 4.52 (d, $J = 12.0$ Hz, 1H), 4.64 (d, $J = 12.0$ Hz, 1H), 4.71 (s, 2H), 5.57 (d, $J = 0.9$ Hz, 1H), 7.30–7.44 (m, 10H); ^{13}C NMR (127.5 MHz, $CDCl_3$): $\delta = 57.78$, 67.94, 68.21, 70.74, 70.96, 72.05, 72.09,74.32, 76.43, 103.65, 127.92, 128.25, 128.35, 128.40, 128.72, 128.91, 138.14, 138.31; HREIMS: *m/z* calcd for $C_{42}H_{44}O_6$ 385.1646 $[M+H^+]$; found 385.1642; elemental analysis: calcd (%) for $C_{22}H_{24}O_6$: C 68.74, H 6.29; found: C 67.63, H 6.09.

(±)-1,2,3,5,6-Penta-O-benzyl-4-O-methyl-myo-inositol (**9**). Dichloromethane (25 μL) was used to dissolve **8** (0.10 g, 0.26 mmol) at room temperature. The solution was diluted with methanol (3 mL) and Dowex 50W-X8–100 (H^+ form, 0.5 g) was added. The suspension was stirred for 14 h after which TLC confirmed completion of the reaction. The resin was removed by filtration and the resulting solution evaporated to yield a colourless oil. The oil was dissolved in dichloromethane and evaporated three times to ensure removal of the methanol. Without further purification, the crude oil was dissolved in dry DMF (1 mL) and sodium hydride (49 mg of a 60% dispersion in oil, 0.11 mmol; ***CAUTION!*** evolution of hydrogen gas) was added. The reaction was stirred for five minutes after which benzyl bromide (0.2 mL, 2 mmol) was added dropwise followed by

continuous stirring for 14 h. The DMF was removed in vacuo to yield an orange oil that was purified by flash chromatography (silica gel, 100% toluene to EtOAc/toluene 1:6, *v/v*) to yield **9** as a white solid (0.165 g, 0.25 mmol, 95% yield). mp 72–74 °C; ^{1}H NMR (500 MHz, $CDCl_3$): $\delta = 3.33$ (dd, $J = 9.85$ Hz, 2.11 Hz, 1H), 3.40 (dd, $J = 2.08$, 9.83 Hz, 1H,), 3.45 (t, $J = 9.19$ Hz, 1H), 3.74 (s, 3H), 3.86 (t, 9.49 Hz, 1H), 4.07 (m, 1H), 4.11 (t, $J = 9.51$ Hz, 1H), 4.63–4.73 (m, 5H), 4.88–4.98 (m, 5H), 7.33–7.46 (m, 25H); ^{13}C NMR (127.5 MHz, $CDCl_3$): $\delta = 61.80$, 72.56, 73.16, 73.21, 74.48, 74.88, 76.28, 76.31, 81.29, 81.35, 84.11, 84.34, 127.75, 127.89, 127.94, 127.96, 128.00, 128.03, 128.23, 128.38, 128.51, 128.57, 128.75, 128.78, 128.82, 128.86, 138.86, 139.03, 139.37, 139.42; HREIMS: *m/z* calcd for $C_{42}H_{44}O_6$ 667.3030 $[M+Na]^+$; found 667.3031; elemental analysis: calcd (%) for $C_{43}H_{44}O_6$: C, 78.23, H 6.88; found: C 78.05; H 6.87.

(±)-1,3,5,6-Tetra-O-*benzyl-4*-O-*methyl*-myo-*inositol* (***10***). An identical procedure was followed as described above for compound **6**. A solution of **9** (0.10 g, 0.16 mmol) gave pure **10** (0.051 g, 0.09 mmol, 58% yield) as a colourless oil. ^{1}H NMR (500 MHz, $CDCl_3$) $\delta = 2.45$ (s, 1H), 3.30 (dd, $J = 2.60$, 7.03 Hz, 1H), 3.36–3.40 (m, 2H), 3.69–3.74 (m, 4H), 3.97 (t, $J = 9.54$ Hz, 1H), 4.03 (m, 1H), 4.71–4.80 (m, 4H), 4.87–4.92 (m, 4H), 7.33–7.40 (m, 20H); ^{13}C NMR (127.5 MHz, $CDCl_3$): $\delta = 61.83$, 68.11, 73.11, 73.18, 76.30, 76.33, 80.07, 80.12, 81.47, 83.47, 83.69, 127.88, 127.96, 127.99, 128.18, 128.23, 128.25, 128.27, 128.38, 128.40, 128.75, 128.76, 128.87, 138.36, 138.52, 139.16, 139.19; HREIMS: *m/z* calcd for $C_{35}H_{38}O_6$: 555.2747 $[M+H]^+$; found: 555.2754; elemental analysis: calcd for $C_{35}H_{38}O_6$: C 75.79, H 6.91; found: C 75.63; H 6.90.

(±)-2,4,5,6-Tetra-O-*benzyl-3*-O-*methyl-1-azido-1-deoxy*-scyllo-*inositol* (***11***). A stirring solution of **10** (0.061 g, 0.11 mmol) in pyridine (1 mL) was lowered partially into an ice bath. Methanesulfonyl chloride (~0.2 mL) was added dropwise and the reaction allowed to gradually reach room temperature. After stirring for 20 h the solution was poured into ice water (1 mL), partitioned and the organic layer further extracted with water (2×1 mL), brine (2×1 mL) and dried (Na_2SO_4). Upon evaporation a yellowish oil remained that was redissolved in CH_2Cl_2 and evaporated once more. Without further purification, the oil was dissolved in DMF (1 mL) and treated with NaN_3 (0.055 g, 0.8 mmol) and heated at 90 °C for 16 h. The DMF was removed in vacuo to yield a solid that was dissolved in ethyl acetate (2 mL) and washed with water (1 mL), brine (1 mL) and dried ($MgSO_4$). Upon evaporation, a yellowish oil remained that was purified by flash chromatography (silica gel, EtOAc/hexane 1:5, *v/v*) to give pure **20** as a gummy solid (0.040 g, 0.07 mmol, 62% yield). ^{1}H NMR (500 MHz, $CDCl_3$): $\delta = 3.26$–3.27 (m, 2H), 3.32 (t, $J = 9.3$ Hz, 2H), 3.53 (t, $J = 9.0$ Hz, 1H), 3.43–3.45 (m, 1H), 3.69 (s, 3H), 4.85 (m, 8H), 7.32–7.47 (m, 20H); ^{13}C NMR (127.5 MHz, $CDCl_3$): $\delta = 61.56$, 61.73, 75.95, 76.00, 76.04, 81.13, 81.01, 82.68, 83.16, 127.78, 127.88, 129.99, 128.16, 128.31, 128.45, 128.51, 128.53, 128.56, 137.83, 137.90, 138.36; IR: $\nu_{N3} = 2107$ cm^{-1}; elemental analysis: calcd (%) for $C_{35}H_{37}N_3O_5$: C 72.52, H 6.43, N 7.25; found: C 72.48, H 6.49, N 7.05.

(±)-3-O-*Methyl*-scyllo-*inosamine* (***2***). An identical procedure was followed as described above for compound **1.** Azide **11** (0.082 g, 0.14 mmol) produced **2** as the hydrochloride salt (0.026 g, 0.11 mmol, 78% yield). ^{1}H NMR (500 MHz, D_2O): $\delta = 3.01$ (t, $J = 10.6$ Hz, 1H), 3.11 (t, $J = 8.8$ Hz, 1H), 3.32 (m, 2H), 3.38 (m, 1H), 3.52 (m, 4H); ^{13}C NMR (127.5 MHz, D_2O): $\delta = 56.16$, 60.80, 69.82, 70.17, 72.85, 74.59, 84.52. HREIMS: *m/z* calcd for $C_7H_{15}NO_5$: 194.1023 $[M+H]^+$; found 194.1028.

Enzyme assays: Purification of recombinant MosA has been described previously.[18] Centrifugation was performed using either a Beckman–Coulter microfuge 18 and 22R centrifuge or a Beckman J2-HS refrigerated centrifuge with a JLA-10.5 or JA-25.5 rotor. Cultures were grown in an Innova 4230 incubator shaker and were lysed with a Virosonic 600 ultrasonic cell disrupter. A BioCAD Sprint Perfusion Chromatography system was routinely used for large scale protein purifications. Protein concentrations were determined using the Bio-Rad Bradford assay kit following manufacturers instructions, with BSA as a standard for calibration. UV-visible spectrophotometry was performed on a Beckman DU-640 spectrophotometer with a circulating-bath-controlled temperature block. Assays were performed in a 1 mL cuvette containing imidazole buffer (100 mM, pH 7.7), K_2HPO_4 (10 mM), MosA (52 nM, based on monomer weight of 33341 g mol^{-1}) while maintaining a temperature of 37 °C. Reaction progress was monitored spectrophotometrically at 270 nm (following the formation of dipicolinate with $\varepsilon_{270} = 4000$ M^{-1} cm^{-1}), as described by Borthwick et al.[49] All data represent the average of at least two experiments. Kinetic constants were determined as described previously.[18]

Inhibition assays were performed as in the kinetic assays described above with the exception that 2-oxobutyrate was added and the solution incubated at 37 °C for 2 min prior to the initiation of the reaction with pyruvate. Four different concentrations of 2-oxobutyrate were used (4, 1.5, 1.0, and 0.25 mM) while varying pyruvate concentrations (0.125, 0.25, 0.5, 1, and 1.5 mM) and keeping ASA concentrations constant (0.23 mM). Rhizopine inhibition experiments were performed similarly, with different concentrations of *scyllo*-inosamine (0.5, 2, 4, and 10 mM) while keeping constant concentrations of pyruvate (0.5 mM).

Imine trapping experiments: Three microcentrifuge tubes containing 160 μL of imidazole buffer (100 mM imidazole, 10 mM KH_2PO_4, pH 7.2) and MosA (40 μL of 2.6 mg/mL, 3.11 nmol) were prepared and kept on ice. A solution of pyruvate (800 mM), and a solution of 2-oxobutyrate (800 mM) were prepared in the same buffer. One sample labelled as the control had 2.35 μL of imidazole buffer added to it. The other two samples had 2.35 μL of the pyruvate solution (1.88 μmol) or 2.35 μL of the 2-oxobutyrate (1.88 μmol) solution added to them. After incubation of all three for 15 min at room temperature, freshly dissolved $NaBH_4$ (2.25 μL, 500 mM, 1.13 μmol) in cold water was introduced and the reaction allowed to sit for 1 h on ice. After this time water (100 μL) was added and the entire solution concentrated and desalted in a Pall centrifugal concentrator. Water (100 μL) was used to dissolve the protein from the membrane and 30 μL of this was injected into a Waters 2796 Alliance Bio HPLC fitted with a C4 Symmetry 300 column (2.1×100 μm, 3.5 μm partical size) with UV detection at 280 nm. Mobile phases were solvent A (water with TFA, 0.1% *v/v*) and solvent B (acetonitrile with TFA, 0.1% *v/v*) set to the following timetable : $T_{0\,min}$ 95% A, 5% B to $T_{15\,min}$ 30% A, 70% B (gradient), $T_{15.01\,min}$ to $T_{25\,min}$ 95% A, 5% B (direct). The flow rate was set at 0.5 mL min^{-1} with a column temperature of 40 °C. The HPLC was fitted with a flow splitter that allowed injection of eluent into a LCT Micromass mass spectrometer.

Inactivation of the enzyme was assessed in samples treated as above except that prior to concentration of the protein, the solution was dialysed overnight into imidazole buffer (100 mM imidazole, 10 mM KH_2PO_4, pH 7.2). The protein activity was then assayed as described above.

Analysis of reaction mixtures by HPLC: All separations were performed with an Agilent 1100 system. To investigate 2-oxobutyrate as a methyl donor, reaction mixtures were prepared containing **1** (5 mM), 2-oxobutyrate (5 mM), MosA (0.5 μM) in phosphate buffer

(0.1 M, pH 7.0) to a final volume of 1 mL. Reactions were incubated at 37 °C with 250 μL samples removed for analysis after 1, 2 and 3 h. Prior to derivatization, protein was removed by a Pall Life Science centrifugal concentrator following manufacturer's instructions. A 100 μL sample of the filtrate was mixed with 9-fluorenylmethyl chloroformate (100 μL, 5 mM solution in acetonitrile) and allowed to react for 15 min at room temperature. A 10 μL aliquot of the reaction mixture was injected into an HPLC fitted with a Zorbax C8 reverse phase column (250 mm × 4.6 mm I.D., 5 μm particle size) pre-equilibrated with 70% deionized H_2O and 30% acetonitrile. A solvent gradient to 100% acetonitrile over 12 min eluted the derivatized rhizopines. The mobile-phase flow rate was 1.0 mL min^{-1}, with the column temperature set at 25 °C and UV detector at 254 nm.

To investigate SAM as a methyl donor, reaction mixtures were prepared with SAM (2.5 mM), **1** (2.5 mM), MosA (0.23 μM) to a final volume of 1 mL in imidazole buffer (100 mM imidazole, 10 mM KH_2PO_4, pH 7.6). A control reaction included all above reagents except MosA. Both reactions were incubated at 37 °C with 250 μL samples removed for analysis after 1, 2 and 3 h. Prior to analysis, protein was removed by a Pall Life Science centrifugal concentrator following manufacturer's instructions. A 10 μL injection of the reaction mixture was injected into an HPLC fitted with a Zorbax C18 reversed-phase column (250 mm×4.6 mm i.d., 5 μm particle size) pre-equilibrated with 25% MeOH and 75% buffer (8 mM $CH_3(CH_2)_6SO_4Na$, 40 mM $NH_4H_2PO_4$, pH 3.0) at a flow rate of 1.0 mL min^{-1}, column temperature of 25 °C and UV detector set at 260 nm.

To demonstrate the detection of methyl transfer using catechol *O*-methyltransferase (COMT), reactions were performed in phosphate buffer (200 mM NaH_2PO_4, 5 mM $MgCl_2$, pH 7.4), COMT (100 units—one unit is the amount of enzyme that can catalyze the methylation of 1 nmol of 3,4-dihydroxybenzoic acid per hour at 37 °C), SAM (3 mM), and 3,4-dihydroxybenzoic acid (2 mM). A reaction assay containing everything above except enzyme was used as a control. Both reactions were kept at 37 °C for 2.5 h after which protein was removed by a Pall Life Science centrifugal concentrator following manufacturer's instructions. A 10 μL sample was injected into the HPLC as described above.

Protein crystallography: Conditions for crystallization have been described previously.[50] Crystals were screened over a variety of conditions with many conditions producing crystals. Crystals used in diffraction were grown using a well solution of ammonium sulfate (2 M), Tris buffer (100 mM), and polyethyleneglycol 400 (PEG400, 2% *v/v*). The well solution was then mixed with the protein solution in a 1:1 ratio and crystals grew overnight. Crystals were then harvested and soaked in a cryoprotectant solution consisting of ammonium sulfate (2 M), Tris buffer (100 mM), PEG400 (2% *v/v*), glycerol (10%), pyruvate (100 mM), and L-lysine (100 mM). Crystals were soaked for 10 min and then flash cooled in liquid nitrogen. X-ray data were collected at the Canadian Light Source beamline 08ID-1 for MosA crystals soaked with pyruvate and L-lysine. Two data sets were collected in a nitrogen stream at 105 K using a MAR225 CCD detector. For both data sets, 360 images were collected with 0.5° oscillation per image around the omega axis. A wavelength of 1.3 Å was used. The crystals diffracted to 2.2 Å and 1.95 Å, but the data for the former did not index properly. The 1.95 Å data were indexed using XDS and then integrated using Mosflm.[51] These data were finally scaled using Scala from the CCP4 suite of programs.[33] Final coordinates of MosA have been deposited with accession number 2VC6 in the RSCB Protein Databank (http://www.rcsb.org/pdb/).

Isothermal titration microcalorimetry: ITC measurements were performed on a CSC ITC-4200 (Calorimetry Sciences Corp., Lindon Utah) calorimeter. Purified MosA was dialyzed exhaustively against assay buffer (100 mM imidazole, 10 mM K_2HPO_4 pH 7.7) at 5 °C. A portion of the dialysate was saved for preparation of the ligand solutions. Protein concentrations were determined immediately before use as described above, and the enzyme assayed to ensure that it was fully active. All solutions were degassed under vacuum for a period of at least 10 min immediately prior to their use. A typical experiment involved 20 injections of 5 μL ligand solution (50 mM) into a sample cell containing 1.30 mL of protein solution (ca. 0.1 mM) after a stable baseline had been achieved. The sample cells were continuously stirred at 300 rpm with 3.5 min intervals between injections. Dilution heats were determined by the area of each injection peak after saturation and subtracted from each injection. ITC data was analyzed by Bindworks 1.0 with the independent and cooperative binding models included in the software. The independent model in which the analytical solution for the total heat is [Eq. (1)]:

$$Q = \mathrm{V} \cdot \Delta H \cdot \left[[\mathrm{L}] + \frac{1 + [\mathrm{M}] \cdot n \cdot K - \sqrt{(1 + [\mathrm{M}] \cdot n \cdot K - [\mathrm{L}] \cdot K)^2 + 4K \cdot [\mathrm{L}]}\}}{2K} \right] \quad (1)$$

where V is the total volume, ΔH is the enthalpy of association, K is the binding constant, n is the number of binding sites, [M] is the concentration of the macromolecule, and [L] is the concentration of the ligand. A binding stoichiometry of 1.0 was input into software prior to the curve fitting for titrations with pyruvate and with 2-oxobutryate.

Acknowledgements

This work was supported by a Discovery Grant from the Natural Sciences and Engineering Research Council of Canada (NSERC) and a Research Innovation Award (RI0532) from Research Corporation to D.R.J.P., and by an NSERC Discovery Grant to L.T.J.D. who is a Tier 1 Canada Research Chair in Structural Biochemistry. C.P.P. was supported by an NSERC postgraduate scholarship and an award from the Indigenous Peoples Health Research Centre. K.N. was supported by a scholarship from the Saskatchewan Synchrotron Institute. The authors thank the Saskatchewan Health Research Foundation for funding the Molecular Design Research Group of the University of Saskatchewan. The authors thank Dr. Ron Verrall for helpful discussions; Dr. David Sanders (Department of Chemistry, University of Saskatchewan) for access to the BioCAD and for helpful discussions; and Ken Thoms and Jason Maley (Saskatchewan Structural Sciences Centre), Karen Molochuk (Saskatoon Cancer Centre), and Michel Fodje (Canadian Light Source) for technical contributions. The Canadian Light Source is supported by NSERC, the National Research Council, the Canadian Foundation for Innovation, and the University of Saskatchewan.

Keywords: inhibitors · isothermal titration microcalorimetry · rhizopine · Schiff bases · synthases

[1] E. M. Lodwig, A. H. F. Hosie, A. Bordes, K. Findlay, D. Allaway, R. Karunakaran, J. A. Downie, P. S. Poole, *Nature* **2003**, *422*, 722–726.
[2] J. Sprent, *New Phytol.* **2007**, *174*, 11–25.
[3] P. J. Murphy, W. Wexler, W. Grzemski, J. P. Rao, D. Gordon, *Soil Biol. Biochem.* **1995**, *27*, 525–529.
[4] P. J. Murphy, N. Heycke, S. P. Trenz, P. Ratet, F. J. Debruijn, J. Schell, *Proc. Natl. Acad. Sci. USA* **1988**, *85*, 9133–9137.
[5] P. J. Murphy, S. P. Trenz, W. Grzemski, F. J. Debruijn, J. Schell, *J. Bacteriol.* **1993**, *175*, 5193–5204.
[6] P. J. Murphy, N. Heycke, Z. Banfalvi, M. E. Tate, F. Debruijn, A. Kondorosi, J. Tempe, J. Schell, *Proc. Natl. Acad. Sci. USA* **1987**, *84*, 493–497.
[7] M. C. Lawrence, J. A. R. G. Barbosa, B. J. Smith, N. E. Hall, P. A. Pilling, H. C. Ooi, S. M. Marcuccio, *J. Mol. Biol.* **1997**, *266*, 381–399.
[8] P. C. Babbitt, J. A. Gerlt, *J. Biol. Chem.* **1997**, *272*, 30591–30594.
[9] S. Blickling, C. Renner, B. Laber, H. D. Pohlenz, T. A. Holak, R. Huber, *Biochemistry* **1997**, *36*, 24–33.
[10] G. Scapin, J. S. Blanchard, *Advances in Enzymology, Vol. 72* **1998**, p. 279.
[11] R. C. J. Dobson, S. R. A. Devenish, L. A. Turner, V. R. Clifford, F. G. Pearce, G. B. Jameson, J. A. Gerrard, *Biochemistry* **2005**, *44*, 13007–13013.
[12] R. C. J. Dobson, J. A. Gerrard, F. G. Pearce, *Biochem. J.* **2004**, *377*, 757–762.
[13] R. C. J. Dobson, M. D. W. Griffin, G. B. Jameson, J. A. Gerrard, *Acta Crystallogr. Sect. D Biol. Crystallogr.* **2005**, *61*, 1116–1124.
[14] R. C. J. Dobson, M. D. W. Griffin, S. J. Roberts, J. A. Gerrard, *Biochimie* **2004**, *86*, 311–315.
[15] R. C. J. Dobson, K. Valegard, J. A. Gerrard, *J. Mol. Biol.* **2004**, *338*, 329–339.
[16] J. J. Turner, J. A. Gerrard, C. A. Hutton, *Bioorg. Med. Chem.* **2005**, *13*, 2133–2140.
[17] J. J. Turner, J. P. Healy, R. C. J. Dobson, J. A. Gerrard, C. A. Hutton, *Bioorg. Med. Chem. Lett.* **2005**, *15*, 995–998.
[18] P. H. Tam, C. P. Phenix, D. R. J. Palmer, *J. Mol. Biol.* **2004**, *335*, 393–397.
[19] P. Lestrate, A. Dricot, R. M. Delrue, C. Lambert, V. Martinelli, X. De Bolle, J. J. Letesson, A. Tibor, *Infect. Immun.* **2003**, *71*, 7053–7060.
[20] C. P. Saint, M. Wexler, P. J. Murphy, J. Tempe, M. E. Tate, P. J. Murphy, *J. Bacteriol.* **1993**, *175*, 5205–5215.
[21] P. M. Flatt, T. Mahmud, *Nat. Prod. Rep.* **2007**, *24*, 358–392.
[22] T. J. Donohoe, P. D. Johnson, R. J. Pye, M. Keenan, *Org. Lett.* **2005**, *7*, 1275–1277.
[23] P. Serrano, J. Casas, M. Zucco, G. Emeric, M. Egido-Gabas, A. Llebaria, A. Delgado, *J. Comb. Chem.* **2007**, *9*, 43–52.
[24] L. Anderson, H. A. Lardy, *J. Am. Chem. Soc.* **1950**, *72*, 3141–3147.
[25] G. I. Drummond, J. N. Aronson, L. Anderson, *J. Org. Chem.* **1961**, *26*, 1601–1607.
[26] T. Suami, F. W. Lichtenthaler, S. Ogawa, *Bull. Chem. Soc. Jpn.* **1966**, *39*, 170–178.
[27] M. Egido-Gabás, P. Serrano, J. Casas, A. Llebaria, A. Delgado, *Org. Biomol. Chem.* **2005**, *3*, 1195–1201.
[28] J. B. Walker, M. S. Walker, *Biochemistry* **1967**, *6*, 3821–3829.
[29] J. B. Walker, *Appl. Environ. Microbiol.* **2002**, *68*, 2404–2410.
[30] A. Krief, W. Dumont, D. Billen, J. J. Letesson, P. Lestrate, P. J. Murphy, D. Lacroix, *Tetrahedron Lett.* **2004**, *45*, 1461–1463.
[31] S. Koto, M. Hirooka, T. Yoshida, K. Takenaka, C. Asai, T. Nagamitsu, H. Sakuma, M. Sakurai, S. Masuzawa, M. Komiya, T. Sato, S. Zen, K. Yago, F. Tomonaga, *Bull. Chem. Soc. Jpn.* **2000**, *73*, 2521–2529.
[32] V. N. Azev, M. d'Alarcao, *J. Org. Chem.* **2004**, *69*, 4839–4842.
[33] Collaborative Computational Project, Number 4, *Acta Crystallogr. Sect. D Biol. Crystallogr.* **1994**, *50*, 760–763.
[34] R. A. Laskowski, M. W. Macarthur, D. S. Moss, J. M. Thornton, *J. Appl. Crystallogr.* **1993**, *26*, 283–291.
[35] M. A. Perugini, M. D. W. Griffin, B. J. Smith, L. E. Webb, A. J. Davis, E. Handman, J. A. Gerrard, *Eur. Biophys. J.* **2005**, *34*, 469–476.
[36] L. Holm, J. Park, *Bioinformatics* **2000**, *16*, 566–567.
[37] R. J. Cox, *Nat. Prod. Rep.* **1996**, *13*, 29–43.
[38] W. E. Karsten, *Biochemistry* **1997**, *36*, 1730–1739.
[39] M. Dixon, *Biochem. J.* **1953**, *55*, 170–171.
[40] B. Laber, F. X. Gomisruth, M. J. Romao, R. Huber, *Biochem. J.* **1992**, *288*, 691–695.
[41] X. L. Zhu, J. B. Cai, J. Yang, Q. D. Su, *Carbohydr. Res.* **2005**, *340*, 1732–1738.
[42] R. Talhout, A. Villa, A. E. Mark, J. B. F. N. Engberts, *J. Am. Chem. Soc.* **2003**, *125*, 10570–10579.
[43] A. Velazquez-Campoy, E. Freire, *Biophys. Chem.* **2005**, *115*, 115–124.
[44] S. Leavitt, E. Freire, *Curr. Opin. Struct. Biol.* **2001**, *11*, 560–566.
[45] W. B. Turnbull, A. H. Daranas, *J. Am. Chem. Soc.* **2003**, *125*, 14859–14866.
[46] A. P. Brogan, W. R. Widger, D. Bensadek, I. Riba-Garcia, S. J. Gaskell, H. Kohn, *J. Am. Chem. Soc.* **2005**, *127*, 2741–2751.
[47] S. J. Roberts, J. C. Morris, R. C. J. Dobson, C. L. Baxter, J. A. Gerrard, *Arkivoc* **2004**, 166–177.
[48] D. C. Billington, R. Baker, J. J. Kulagowski, I. M. Mawer, J. P. Vacca, S. J. Desolms, J. R. Huff, *J. Chem. Soc. Perkin Trans. 1* **1989**, 1423–1429.
[49] E. B. Borthwick, S. J. Connell, D. W. Tudor, D. J. Robins, A. Shneier, C. Abell, J. R. Coggins, *Biochem. J.* **1995**, *305*, 521–524.
[50] Y. A. Leduc, C. P. Phenix, J. Puttick, K. Nienaber, D. R. J. Palmer, L. T. J. Delbaere, *Acta Crystallogr. Sect. F Struct. Biol. Cryst. Commun.* **2006**, *62*, 49–51.
[51] A. Leslie in *MOSFLM Users Guide*, MRC Laboratory of Molecular Biology, Cambridge, **1995**.

Received: September 23, 2007
Published online on June 6, 2008

